SAND2014-4122C

Hardness Assurance in Advanced Semiconductor Packaging with ^{85}Kr Leak Testing

Gary K. Lum[1], David Beutler[2], Dolores Walters[3] and William P. Ballard[4]

Lockheed Martin Space Systems Company[1], MannaTech Engineering, LLC[2], L3 Applied Technologies[3], Sandia National Laboratories[4]

FOR REVIEW USE ONLY

Corresponding and Presenting Author:
Gary K. Lum, Lockheed Martin Space Systems Company, Sunnyvale, CA 94088 (USA),
Phone: 408-756-0120, email: gary.lum@lmco.com

Contributing Authors:
David Beutler, MannaTech Engineering, LLC, Albuquerque, NM, USA
Email: debeutler@drmtengineering.com

Dolores Walters, L3 Applied Technologies, San Diego, CA, USA
Phone: 858-404-7883, email: Dolores.Walters@l-3com.com

William P. Ballard, Sandia National Laboratories, Livermore, CA, USA
Phone: 925-294-3684, email: wpballa@sandia.gov

Hardness Assurance in Advanced Semiconductor Packaging with ^{85}Kr Leak Testing

Gary K. Lum, *Senior Member, IEEE*, David Beutler, Dolores Walters and William P. Ballard, *Senior Member, IEEE*

***Abstract* – This paper provides an explanation for the significant gain degradation observed from ^{85}Kr leak testing of a bipolar discrete transistor and raises a hardness assurance concern in the leak testing of advanced hermetic semiconductor packaging. A model was developed which explains this response using radiation transport simulations. Results from the model also explain why failures would not be observed if the thickness of the lid was increased. By detailed examination of how the leak test was performed, our model further explains why only about 20% of the parts would exhibit large gain degradations while 80% of the parts would show little, if any, hfe gain degradation. Other electrical parameters of 2N2907 may degrade also, but to a lesser degree. Hardness assurance and hardening methods of mitigating this concern are discussed.**

Index Terms–**^{85}Kr leak testing, bipolar, total ionizing dose, electrons, betas, ceramic packaging**

I. INTRODUCTION

As military acquisition demands the use of commercial electronic products in military systems, the need for high reliability parts continues to rise. Although affordability reasons drive the need for plastic encapsulated parts, there still will be a need for hermetically sealed qualified parts in various applications. Popular leak tests developed over the past decades for qualifying semiconductor devices, such as the bubble or helium (He) techniques are limited in their sensitivity for leak detection and are time consuming, limited to perhaps 300 parts per hour. An alternative method has tremendous testing advantages with over a 100 times faster test rate and higher accuracy. The technique uses radioactive ^{85}Kr instead of He. Parts are placed into a pressurized ^{85}Kr and air mixture for several hours to allow the radioactive gas to penetrate into the potentially leaky parts.

The portion of this work performed at Sandia National Laboratories was supported by the U. S. Department of Energy. Sandia National Laboratories is a multi-program laboratory managed and operated by Sandia Corporation, a wholly owned subsidiary of Lockheed Martin Corporation, for the U.S. Department of Energy's National Nuclear Security Administration under contract DE-AC04-94AL85000.

Gary K. Lum, Lockheed Martin Space Systems Co., Sunnyvale, CA, email: gary.lum@lmco.com
David Beutler, MannaTech Engineering, LLC, Albuquerque, NM, USA, email: debeutler@drmtengineering.com
Dolores Walters, L3 Applied Technologies, San Diego, CA, USA email: Dolores.Walters@l-3com.com
William P. Ballard, Sandia National Laboratories, Livermore, CA, USA, email: wpballa@sandia.gov

The exposed parts are then removed from the pressure chamber and scanned for any residual ^{85}Kr leaking from within the part cavity. This technique is becoming popular because it can examine parts faster. The minimum leak-rate detection level is 10^7 times greater than the He approach and the test can examine 30,000 parts per hour. Because the ^{85}Kr test can test a huge quantity at a time, this test may be used as a 100% screen.

With advances in semiconductor technologies, such as the shrinkage of semiconductor devices, ways are being developed to also scale down the package housing dimensions in the examples shown in Figs. 1 and 2 to incorporate more parts on a printed circuit card. Figs. 1 and 2 plot ceramic lid thickness of moderate size devices and the side- wall thickness of small discrete semiconductor devices for various cavity areas over a die. As the area of a die shrinks, the thickness of the lid and the sidewall are reduced. A strong dependence in the sidewall is observed as the die area shrinks. The smallest lid thickness was 0.023 cm (9 mil) with an area of 0.13 cm^2 (20,164 mil^2). The thinnest wall thickness is about 0.018 cm (7 mil) with an area of 0.019 cm^2 (3000 mil^2). Sidewalls and lids that have thicknesses on the order of 0.025 cm or less have raised a concern when ^{85}Kr is used as a technique for screening for package leaks. An example of this concern can be illustrated with a 2N2907A, pnp discrete bipolar transistor. This discrete transistor is housed in a surface mount UB ceramic package with a 0.025 cm-thick ceramic lid and 0.018 cm-thick sidewall. Although we focused on the UB package, this applies to other ceramic packages of similar geometries as shown in Figs. 1 and 2.

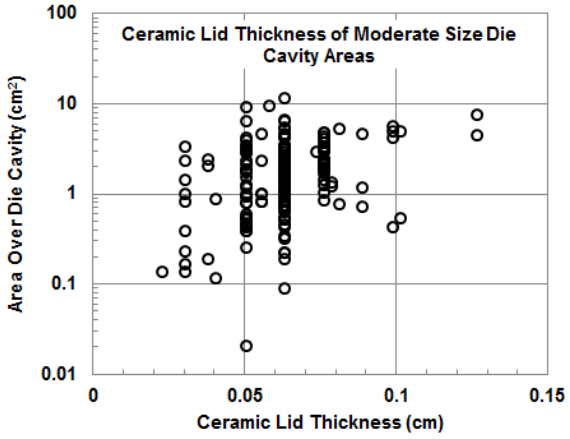

Figure 1. Ceramic lid thickness of moderate package size die cavity areas.

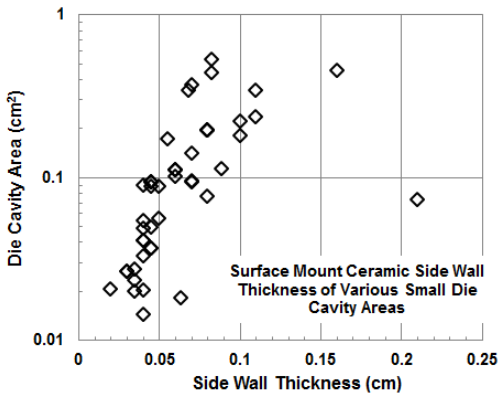

Figure 2. Surface mount ceramic package sidewall thickness versus small die cavity areas in discrete semiconductor devices.

Several assumptions were made to simplify our initial calculations. During the exposure a chamber was pressurized to 6.8 atm of air. Radioactive ^{85}K was then introduced into the chamber to create an air-Krypton mixture with an activity of 250 μCi/(cm^3-atm). The parts are then exposed to ^{85}K for 38.6 hours. Fig. 3 shows a glass vial that housed the 170 parts for the leak test. The UB packaged 2N2907s transistors were removed from their waffle carriers, poured onto a sheet of paper, and then funneled into these glass vials. A glass vial only held parts from a single lot. If the lot contained several hundred of these 2N2907 parts, these parts would be contained in several vials. No attention is paid to stacking the parts in any particular orientation because the pressurized gas used for the leak test will not be affected by their orientation. A metal bucket carrying these vials would then be placed inside a pressurized chamber. The vacuum chamber is about 7.62 cm in radius and 50.8 cm in height.

The vials that held the 170 parts were a #223686 type container manufactured by Wheaton. With a 7.62 cm radius aluminum holder, it could hold a number of these vials. A UB package has the dimensions of 0.325 cm by 0.274 cm or an area of 0.089 cm^2. The glass vial has an internal cross-sectional area of π(1.2 cm)^2 or 4.52 cm^2. Therefore, one glass vial can hold about 4.52 cm^2 / 0.089 cm^2 per UB part = 51 parts in a single layer. At most either one glass vial or two glass vials could hold the 170 parts. With one vial there would be, on average, three to four layers of parts. With two vials, there are about two layers of parts. With one vial, some of the parts will be lying on top of other parts. If the parts were randomly placed into the vial, 50% of the parts will have their lids facing up, while the other 50% will be upside down or partially tilted. If all the parts were placed in one vial, there would be 3 to 4 layers of parts. Only ¼ of the parts would be at the top. Therefore ¼ x 170 parts = 43 parts. If 50% of them are right side up, then 50% of 43 = 21 parts or 12.4% would have their lids facing up. If we assume that the majority of the dose is from the radiation transmitted through the thin lid, then only this small percentage of parts would have been exposed to the ionizing radiation. *This estimate agrees with the 15-20% of parts that were found to exhibit large hfe degradation in the parts that came back from the leak test.*

Table 1. 2N2907 table showing the hfe gain specification limits.

Parameter	Symbol	Conditions		Minimum	Maximum
		Ic (mA)	Vce (V)		
DC Current Gain	hfe1	-0.1	-10	75	-
	hfe2	-1.0	-10	100	450
	hfe3	-10	-10	100	-
	hfe4	-150	-10	100	300

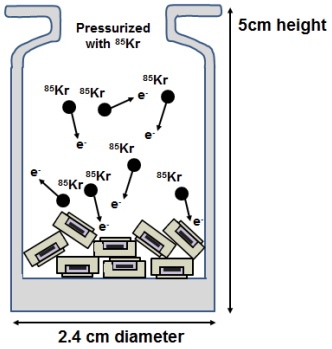

Figure 3. Illustration of a glass vial that held the parts in the ^{85}Kr leak test.

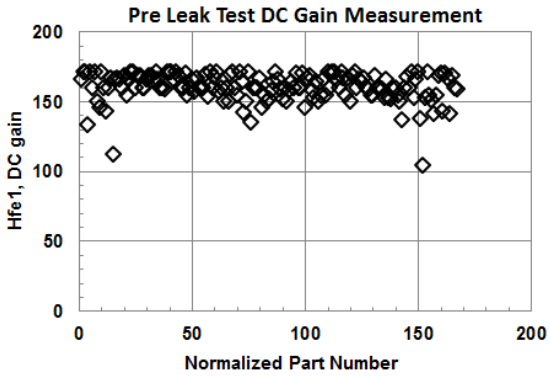

Figure 4. DC gain measurements of the 170 parts from LDC 0908 prior to the leak test.

A ^{85}Kr leak test was initially performed on 170 parts from a single Lot Date Code (LDC), 0908. Fig. 4 shows a plot of the 170-hfe1 measurements prior to the ^{85}Kr leak test. The majority of the parts had hfe1 values tightly clustered between 150 and 170. The ^{85}Kr technique was selected because of the large quantity of parts, better cost effectiveness and efficiency than the traditional helium-leak test method specified in Military Standard 883, test method 1014 or Military Standard 750, test method 1071.7. According to the supplier's final test report which included the original 170 parts, 923 parts passed the fine-leak hermeticity test and only two parts actually failed. When the initial 170 parts which had electrical measurements prior to the leak test were returned for electrical measurements, six parts identified in Fig. 5 (open circles) failed the minimum hfe1 limit of 75 at an I_c current of 100 μA

as described in Table 1. Two of those six parts had low hfe1s prior to the leak test. An additional 21 parts shown in Fig. 5 (solid triangle) exhibited a delta gain reduction (pre leak test – post leak test) of greater than 50. Fig. 5 shows the delta changes in the DC gains before and after the leak test. About 15 to 20% of the parts exhibited large gain changes returning from the leak test, while surprisingly the remaining 80% did not appear to have significant gain degradation. The open circles in Fig. 5 represents 4% of the parts that failed the minimum hfe1 limit specified in Table 1. Initially, speculations focused on the quality of the package lid seal and the electrical measurement techniques, but the results could not provide a comprehensive consistent explanation to (1) why just 15 to 20% were failing and (2) why the hfe degradation was so large in some parts and not in others.

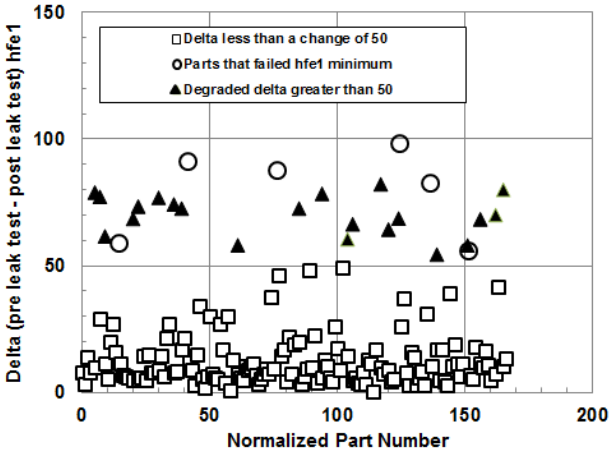

Figure 5. DC gain results between pre leak and post leak test.

Another 719 parts had been tested from 36 other lots. Among these 719 parts, 155 parts failed the hfe1 minimum of 75. Assuming that it is legitimate to combine all the parts that exhibited a large hfe1 change of ≥ 50, the percentage of significant gain degradation would be (6 + 21+ 155)/(170 + 719) = 0.205 or 21% failures. Fig. 5 shows the important message that out of 889 parts that were leak tested only 2 parts were identified showing any noticeable leakage. Eight hundred and eighty seven parts passed the leak test and therefore the effects observed cannot be attributed to the presence of ^{85}Kr within the package. Our hypothesis to explain this degradation, is that betas (electrons), emitted from the radioactive decay of ^{85}Kr inside the pressure chamber, will not all be stopped by the thin 0.025 cm ceramic lid. Some of the betas will penetrate the ceramic lid and deposit a large dose in the passivation layer of the device. This dose causes the hfe1 to degrade and fail the requirement in Table 1.

II. KRYPTON-85 BETA SPECTRUM

The ^{85}Kr beta spectrum had to be determined accurately before performing any radiation transport modeling. Krypton-85 decays into stable Rubidium-85, with a half-life of 10.756 years [3, 4]. The maximum decay energy is 687 keV. The primary decay branch is mostly betas (electrons), about 99.57% electron emission with a maximum energy of 687 keV and an average energy of 251 keV. The second decay branch is 0.43% by beta particle emission at maximum energy of 173 keV followed by gamma ray emission of 514 keV. Since the second decay branch is less than 1%, we assumed that the gamma dose associated with the beta emission is negligible compared to the dose from the betas from the primary decay branch.

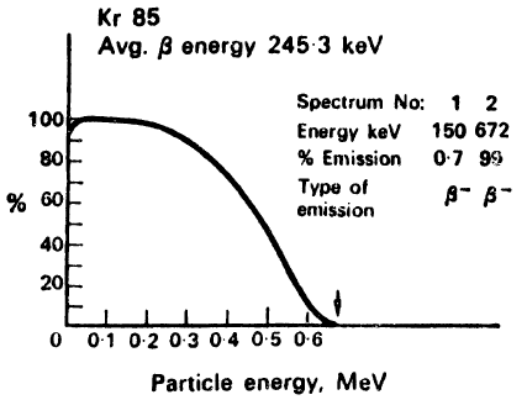

Figure 6. ^{85}Kr beta decay spectrum [3, 4] leak test. Degraded gains are also shown.

A beta spectrum of ^{85}Kr determined experimentally shown in Fig. 6 [3, 4] was originally chosen. The differential energy spectrum can also be obtained analytically from the Fermi theory of beta decay from the following equation [5].

$$dN \propto (T_e^2 + 2T_e m_e c^2)^{1/2}(Q - T_e)^2(T_e + m_e c^2)\ x\ p^2 f(Z', p)\ x\ |M_{fi}^2|\ x\ S(p,q) \quad - \quad (1)$$

where dN is the number of particles, p is the momentum of the beta particle, Q is the decay energy or endpoint energy and T_e is the kinetic energy of the beta particle. The $(T_e^2 + 2T_e m_e c^2)^{1/2}$ x $(T_e + m_e c^2)$ x $(Q - T_e)^2$ term is the fundamental beta equation describing the beta distribution as a function of energy.

The last three terms are refinements to the beta and positron spectra. If p^2 is combined with $(Q - T_e)^2$ this is the statistical factor that represents the number of final states accessible to the emitted betas. As noted the theoretical spectrum drops below 200 keV, if only the basic equation $(T_e^2 + 2T_e m_e c^2)^{1/2}$ x $(T_e + m_e c^2)$ x $(Q - T_e)^2$ is used. One of the important factors that need to be included is the Fermi function. The Fermi function, $f(Z', p)$ term with Z', the atomic number of the daughter nucleus accounts for the influence of the nuclear Coulomb field. The shape of the spectrum is controlled by the Coulomb repulsion or attraction effect of the nucleus on the beta or positron particle. For betas the attraction of the nucleus causes the betas to be predominant at low energies. The $|M_{fi}^2|$ term, called the nuclear transition matrix element, represents the transition from particular initial (i) and final (f) nuclear states. The $S(p,q)$ term accounts for additional beta (p) and neutrino (q) momentum dependence.

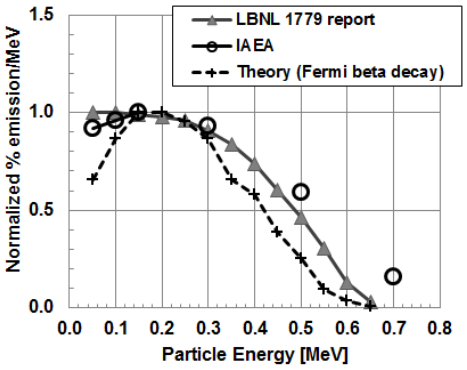

Figure 7. ^{85}Kr beta models.

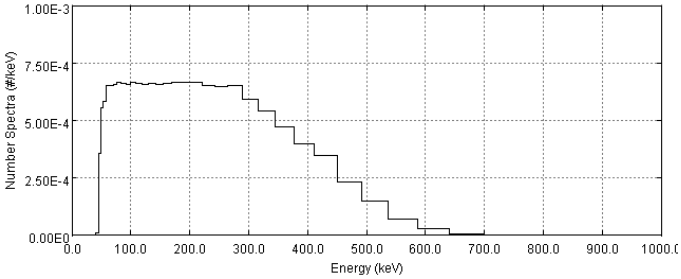

Figure 8. Beta decay spectrum modeled to ^{85}Kr with a peak centered near 245 keV with an endpoint around 672 keV.

To obtain confidence for the correct ^{85}Kr spectrum in Fig. 6 to use in our model, a recent spectrum from IAEA (International Atomic Energy Agency) [7] showed excellent agreement in Fig 7 with the LBNL (Lawrence Berkeley National Laboratory) data. The spectrum does not decrease, but is flat between 50 to 200 keV. We created a spectrum that had an average energy peaked around 251 keV with a maximum energy around 687 keV. Fig. 8 is the ^{85}Kr spectrum that was generated from the 1D radiation transport code, CEPXS/ONEBFP (Coupled Electron Photon Cross Section/One-Dimensional Boltzmann Fokker Planck) for the model.

In the model several assumptions were made.

1) Radioactive ^{85}Kr source is distributed uniformly inside a pressurized vessel
2) Pressurized vessel contained uncapped glass vials with a 1.2 cm radius, 5 cm in height
3) Area of the square die ($3.4\text{x}10^{-3}$ cm^2) has an equivalent circular area with a radius of $3.3\text{x}10^{-2}$ or 0.033 cm
4) Radiation is only important above the die so we can assume that the radiation contribution through other portions of the package was negligible
5) Electrons are attenuated traveling through the 6.8-atm gas
6) ^{85}Kr gamma emission dose is negligible as compared to betas from the radioactivity

Because the transistor was housed in a ceramic housing, we initially assumed that leakage from the sidewalls and the base would be insignificant. The major contribution of the radiation was assumed to be coming through the thin 0.025 cm lid over the chip. Later MCNP5 calculations demonstrated that this assumption was incorrect for the sidewalls if the sidewalls were not shielded by other parts.

The material stack-up in the model included ^{85}Kr, ceramic lid, silicon chip, die attach and back side of the ceramic package. In this stack-up we accounted for air attenuation at 6.8 atm inside the pressurized chamber. The thickness of the ceramic lid was 0.025 cm. The silicon chip was assumed to have 1 μm of thermal oxide to isolate the aluminum metal from the silicon interface. The aluminum metal was 1.5 μm covered by 0.2 μm of silicon nitride (Si_3N_4). The silicon die was 0.025 cm thick.

The analysis was performed in 3 steps. In the first step (a), we transported the ^{85}Kr beta spectrum as shown in Fig. 8 into the silicon die through the ceramic lid. The ^{85}Kr and N_2 gas mixture gas divided in individual slabs whose thickness was defined by the distance from the silicon die inside the vial. The beta spectrum defined by Fig. 8 was transported using CEPXS/ONEBFP through each slab of the gas mixture. The dose deposited in the silicon device was the contribution from each slab. In the second step (b), the electron fluence was determined. Finally in the third step (c), we calculated the solid angle to account for only those electrons produced that would contribute to the dose in the transistor.

III. CEPXS/ONEBFP RESULTS

The 1-D radiation transport code simulated an isotropic environment. The primary betas from krypton are slowed by the 6.8 atm air and most are stopped in the lid. Most of the electrons are deposited in the 0.025 cm ceramic lid. The electrons that pass through the ceramic lid create photon radiation and secondary electrons. Of important interest are layers which represent the Si_3N_4 and SiO_2 layers. These layers are well known for charge trapping, causing gain degradation in bipolar and threshold voltage shifts in MOSFET transistors [7, 8]. In the case of the pnp bipolar transistor, an inversion layer appears at the surface in the region of the base-emitter junction [7]. Surface-recombination current will be generated, increasing the base-emitter leakage current and hence decreasing hfe = $I_{collector}/I_{base}$ or increasing degradation in the DC gain.

The CEPXS/ONEBFP radiation transport code was used to determine the role of bremsstrahlung and secondary electrons in depositing dose in the active layer of the devices that were subjected to leak testing with ^{85}Kr in 6 atm air. At issue was whether or not the dose deposited in the device (represented by a silica layer) was dominated by primary ^{85}Kr betas rather than secondary electrons from bremsstrahlung. The analysis concluded that the primary electrons from ^{85}Kr penetrating the lid of the device dominated the dose deposition at the device. We further showed that the primary electrons dominated the dose through the 0.025 cm silicon chip and that the result is sensitive to the electron incidence angle distribution.

CEPXS/ONEBFP was executed in four different ways: 1) *Full coupling*—betas create photons and both create secondary electrons; 2) *Partial coupling*—betas create photons but photons do not create secondary electrons (dose deposited locally); 3) *No coupling*—betas do not create photons; 4) *No secondary electrons*—secondary electrons are not transported—primary electrons and photons deposit energy locally rather than allowing secondary electrons to carry away energy. It was found that when secondaries are not considered, there is not much difference in the dose computed for the device (layer 5 in **Error! Reference source not found.**11). The main differences occur in the dose deposited in layers below the silicon chip (layer 6), beginning with titanium (layers 8-12). If the energy that would have gone into bremsstrahlung production is thrown out, dose deposition in the gold and silver layers is greatly underestimated. By the time the radiation gets halfway into the alumina base, most of the dose comes from bremsstrahlung.

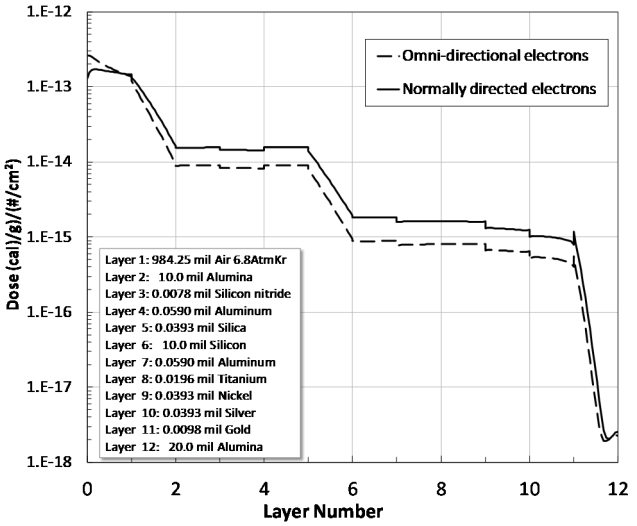

Figure 9. CEPXS/ONEBFP results computed for full coupling, with omni-directional (dash line) or normally directed (solid line) ^{85}Kr electrons. The material stack-up is shown in the inset.

Error! Reference source not found.9 shows the results for the full coupling cases for the variation of electrons that are omni-directional (likely representative of the ^{85}Kr leak test environment) versus normal incident. Up to 2X more dose is deposited in the device for a normally incident beta source. In all cases examined, the betas dominate the dose in the device and penetrate several mils deep. In addition to angle of incidence, variations in the beta spectrum are likely to cause differences in dose deposition for this particular stack-up; there are uncertainties and rough energy binning in both theoretical and measured beta spectra. As a final caveat, one can infer uncertainty in the calculated dose from betas when the fluence is below 0.1% of incident, part way through the 0.025 cm silicon chip. One-dimensional analysis is notoriously inadequate for very highly attenuated positions in a "thick" material stack.

The following calculation shows an example of how the energy was calculated when the betas are transported through 2.5 cm of air at 6.8 atm. The air was divided into a number of thin layers to show how much radiation in each layer of air contributed dose into the Si_3N_4 and SiO_2 layers. The height was divided into thin layers from the bottom of the vial to the top and further up. The radiation in each layer was integrated to give the total dose deposited. The energy deposited in the Si_3N_4 and SiO_2 layers is about $8.9\text{x}10^{-15}$ cal/(g-number of electrons per cm^2) for 2.5 cm of pressurized air.

Energy deposited
= $8.9\text{x}10^{-15}$ cal/(g-number of electrons per cm^2) x 4.184 joule/cal x 10^7 erg/joule
= $3.7\text{x}10^{-7}$ erg/(g-number of electrons per cm^2)
= $3.7\text{x}10^{-9}$ x cGy/(number of electrons per cm^2)

At 3 cm the energy deposited is $7.80\text{x}10^{-15}$ cal/(g-number of electrons per cm^2). The average deposited energy at 2.5 cm was the average of the energies at 2.5 and 3 cm or ($3.7\text{x}10^{-9}$ + $3.26\text{x}10^{-9}$)/2 = *$3.48\text{x}10^{-9}$ cGy/(number of electrons per cm^2)*. An integrated dose at 2.5 cm was then calculated by summing all the layers from the part to 2.5 cm. As one gets closer to the source the average dose per layer increases and as one goes further back, the contribution approaches a saturation level in the dose at about 2 to 3 cm. Due to the attenuation of the pressurized air, the background radiation reaches a near constant dose. At 2.5 cm the integrated dose is **$5.27\text{x}10^{-8}$ cGy(Si)/(electrons per cm^2)**.

A. ELECTRON FLUENCE CALCULATION

To calculate the electron fluence (number of electrons per cm^2), the volume contributing to the dose in each slab was divided into two types of volumes. Above 1.1 cm the volume of each slab was treated as cylinders with the radius of the vial and the average thickness of the slab. Below 1.1 cm the volume of each slab was treated as semi-hemispheres with the average thickness of the slab. At 1.1 cm the two volumes were combined to assure an overlap and correct for lost volume. The 1.1 cm height was chosen to be the transition point because it was the closest to the restricting radius of the vessel. The volume was double counted to try to recover the dose lost from the volumes that were lost near the vessel wall when changing from the hemisphere to cylindrical calculation.

B. VOLUME CALCULATION ABOVE 1.1 cm

The vial has a radius of 1.2 cm and a height of 5 cm. The vial was uncapped for the leak test according to supplier. The integrated dose was calculated to 10 cm. The volume of each slab was calculated to be π (1.2cm)^2 x (height$_1$ - height$_2$). Given 1Ci = $3.7\text{x}10^{10}$ disintegrations/s, the exposure time = 38.6 hrs, height$_2$ = 2.5 cm and height$_1$ = 3 cm

The number of electrons within each slab of volume is:
= 250μCi/(cm^3 atm) x 6.8 atm x $3.7\text{x}10^{10}$ disintegrations/s-Ci x 38.6 hrs x 3600 s/hr x π (1.2cm)^2 x (3cm – 2.5cm)

= 1.98×10^{13} disintegrations. For the disintegrations a beta is released 99.57% of the time. We assumed that the number of electrons is 1.98×10^{13} electrons. However, the unit is dimensionless at this point. To obtain the fluence in electrons per cm^2, we assumed that these electrons are focused on the die so the fluence is divided by the area of the die, 3.4×10^{-3} cm^2. The number of electrons over the die is then 1.98×10^{13} disintegrations / die area
= 1.98×10^{13} disintegrations / π (0.033 cm)^2 = 5.8×10^{15} electrons per cm^2 at a height of 2.5 cm.

The dose contributed from the slab at 2.5 cm from the die = average deposited slab energy x electron fluence / cm^2 = 3.48×10^{-9} cGy(Si)/(number of electrons per cm^2) x 5.8×10^{15} electrons per cm^2 = 2.0×10^{7} cGy(Si). *The dose contributed from the slab at 2.5 cm = 2.0×10^{7} cGy(Si)*

C. VOLUME CALCULATION BELOW 1.1 cm

We can repeat the same approach as section b for calculating the dose below 1.1cm. With $height_2$ = 0.5 cm, $height_1$ = 0.75 cm, the dose contributed from the slab at 0.5 cm = 9.6×10^{6} cGy(Si). However, not all the disintegrations contribute to the charge deposited in the part because they are emitted in every direction. To account for this, we consider the solid angle subtended by the die over a sphere whose radius is the height above the part in the vial.

D. SOLID ANGLE CALCULATION

Solid angle $d\Omega$ = area of the die / 4π(average height)^2

At 2.5 cm $d\Omega = \pi\ (0.033\ cm)^2 / [4\pi\ (\ (2.5\ cm + 3\ cm)/2\ )^2\ ] =$
$(0.033\ cm)2 / (4 \times (2.75\ cm)^2) = 3.6 \times 10^{-5}$

Correcting for the solid angle, the dose contributed by the slab at 2.5 cm is 2.0×10^{7} cGy(Si) x 3.6×10^{-5} = 720 cGy(Si).

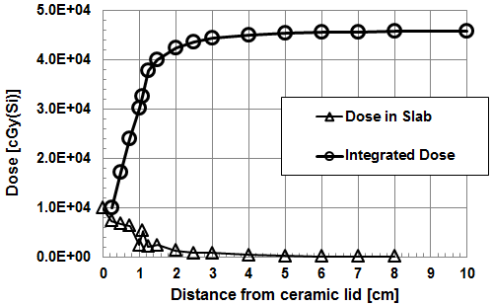

Figure 10. Dose from a slab and the integrated dose at a given distance from the part.

In Fig. 10 the integrated dose predicted by CEPXS/ONEBFP is plotted as a function of distance from the part. At close proximity to the part, the individual dose from each source slab increases to a maximum of 10^{2} Gy(Si) at the surface of the part. As one moves away the dose from each individual source slab decreases. When the dose contribution is integrated over distance, the contribution increases and levels off at approximately 2 cm. At 5 cm, the top of the vial, we obtain a value of 456 Gy(Si). The dose in each slab from larger distances is insignificant.

Fig. 11 is a plot of the DC gain versus collector current of a 2N2907 from Semicoa irradiated with ^{60}Co. According to Fig. 11, at 100 µA of collector current the hfe1 is 28 to 56 for a total dose of 250 to 500 Gy(Si). The degraded gains from Fig. 5 ranged from 44 to 100. We predicted a dose of 456 Gy(Si) at the height of the vial and slightly more beyond the vial to the height of the chamber with the vial uncapped.

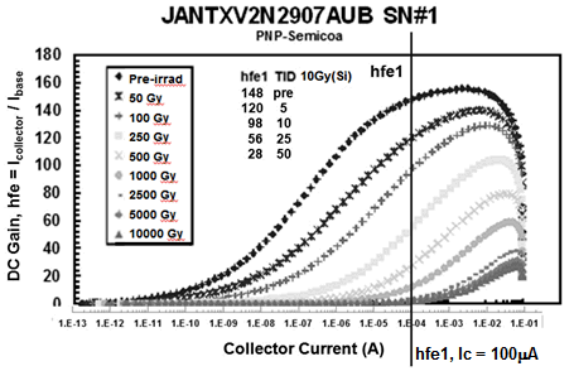

Figure 11. Gain Degradation versus collector at 2.5 cm for current of a 2N2907 irradiated with ^{60}Co.

The energy deposited with a lid that was 0.051 cm (20 mil) thick was calculated to be 996 cGy(Si). According to Fig. 11, 10Gy(Si) gives a hfe1 between 120 to 148. With a minimum requirement of 75, no failures were observed. The prediction confirmed that a 0.051 cm lid will reduce the beta dose to about 10Gy(Si) such that hfe1 parameter will pass. At 0.051 cm virtually no betas were able to penetrate the lid. This supports the hypothesis that parts placed in the vial upside down or up against another part, they would not receive as much dose. Without the shielding from other parts in front of the lid, the part received more dose.

IV. MCNP5 RESULTS

As a check on the more simplistic, one-dimensional estimate, MCNP5 was used to model the three-dimensional radiation transport using an electron source and full electron/photon transport. The glass beaker was modeled as a SiO_2 hollow cylinder with top and bottom end caps, with a 1.2-cm inner radius, 5-cm internal height, and 1-mm wall thickness. A single IC package was located at in the bottom of the beaker on axis. The package was modeled as an Al_2O_3 box constructed from a 3.25-mm x 2.74-mm x 495.7 µm base, a 3.25-mm x 2.74-mm x (254 or 508) µm lid, and a 3.25-mm x 2.74-mm x 670.3 µm rectangular hollow tube with a wall thickness of 165µm. It should be noted that the sidewall is thinner than even the 254-µm lid. This became an important factor in these calculations. The rest of the beaker was filled with 6.8 atm air loaded with 2.88% ^{85}Kr. A 584 µm x 584 µm IC chip was located on top and on axis of the ceramic base of the package. The IC chip is represented as a simple structure with uniform layers that extend from edge to edge. These layers are from bottom to top: 300-nm Au, 1-µm Ag, 1-µm

Ni, 500-nm Ti, 1.5-μm Al, 254-μm Si, 1-μm SiO_2, 1.8-μm Al, 200-nm Si_3N_4. The layer of interest for energy deposition is the SiO_2 layer in the wafer. The rest of the interior of the package is filled with 1 atm of N_2.

The ^{85}Kr electron emission was modeled using the IAEA spectrum, assuming isotropic emission with uniform probability over the entire interior of the interior of the glass beaker except for the volume defined by the IC package and its interior. The total number of electrons emitted from the source was calculated based on the volume, pressure, and activity of the gas and the exposure time. To improve statistics the importance for both photon and electrons was enhanced in the ceramic cells. Obviously, for an electron or photon to deposit energy in the gas, it must first strike the ceramic package, thus only electrons or photons that strike the ceramic will contribute to dose in the SiO_2 layer.

The dose in the SiO_2 layer was calculated using both the F6 dose tally and the F8 pulse height tally. The F6 dose tally provided the dose from photons and the F8 pulse-height dose tally provided the dose due to both photons and electrons. The dose due to photons striking this layer is insignificant compared to the dose from electrons as was discussed elsewhere.

Initially two separate calculations were performed. These were identical except one used a 0.025 cm lid and one used a 0.051 cm lid on the package. The dose for each of the two calculations was significantly larger than the 1-D transport calculations that had been done previously. When the lid thickness was increased, the drop in dose was much less than the 1-D calculations. This result suggested that the dose from electrons entering from the side was significant. As noted earlier the sides are even thinner than the lid. For the 1-D calculations this possibility was ignored and was not considered. However, this model assumes a package in isolation in the middle of the bottom of the beaker, which would exacerbate this effect. When many devices are leak tested simultaneously, the packages will be adjacent to each other and therefore the sides will be shielded.

Table II. 1-D versus 3-D MCNP5 results

Ceramic Lid	1-D CEPXS/ONEBFP	3-D MCNP5
0.0254 cm lid with side leakage	-	924Gy(Si)
0.0508 cm lid with side leakage	-	462Gy(Si)
0.0254 cm lid with no side leakage	456Gy(Si)	498Gy(Si)
0.0508 cm lid with no side leakage	9.96Gy(Si)	68.8Gy(Si)

To simulate this, two more calculations were performed, identical to the first with the exception that both the ceramic sides and base cells were given an importance of 0. This prevented any electrons or photons from entering the package, except through the lid. Both of these calculations agree well with the simple 1-D calculations performed earlier as shown in Table II for the 0.025 cm lid with no side leakage. However, for the 0.051 cm case where straggling becomes important, the angular distribution of the electrons is more difficult to calculate which is why there is a large difference between MCNP5 (3-D Monte Carlo code) and CEPXS/ONEBFP (1-D Discrete Ordinates).

V. DISCUSSION

In the future, there will still be a demand to leak test hermetic sealed ceramic packages in large quantities. Designers may leverage on commercial parts that may have very little radiation hardening, because of the desirability of parts that are cost affordable, small size and can achieve high performance. A design may have to operate in the low collector current range in order to minimize power consumption in a satellite application. In these designs a designer should try to avoid designing with bipolar devices that operate normally with collector currents where the operation can be sensitive to radiation total dose effects. As shown in Fig. 11 DC gains degrade tremendously at low collector current ranges, such as 100 μA or less. Besides the bipolar devices, discrete power MOSFETs with thick gate oxides can be sensitive to total ionizing dose with threshold voltage shifts. The designer could account for the degradation by using multiple gain stages or low voltage MOSFETs with thinner gate oxides. In regards to hardness assurance, care must be taken to assure that if ceramic packaging is required, the lids and sidewalls are no less than 0.051 cm in thickness. Another approach could be to consider the use of higher density Kovar metal lids where 0.025 cm in thickness should prevent the betas from penetrating in. Pre and post ^{85}Kr leak testing electrical measurements should be performed to monitor the amount of DC gain degradation or threshold voltage shift.

VI. CONCLUSION

A radiation transport analysis has been performed to show that a 0.025 cm ceramic lid will allow the deposition of radiation as high as several hundred Gy(Si) during leak testing with ^{85}Kr. Our model explains why only 15 to 20% of the parts exhibited a large amount of degradation while the remaining parts did not exhibit much degradation. This small fraction was due to the parts being randomly placed in a small glass vial in several layers where only the top upward facing parts would be exposed to the betas from ^{85}Kr decay over the height of the vial.

VII. REFERENCES

[1] CEPXS/ONEBFP – Coupled Electron Photon Cross Section/One-Dimensional Boltzmann-Fokker-Planck, radiation code sponsored by the Defense Threat Reduction Agency and the Navy Strategic Systems Program.

[2] MCNP5 – Monte Carlo N-Particle transport code, developed by Los Alamos National Laboratory and distributed by the

Radiation Safety Information Computational Center in Oak Ridge, TN.
[3] "The Beta Ray Spectrum and the Average Beta Energy of Several Isotopes of Interest in Medicine and Biology," J. Mantel, p. 407, International Journal of Applied Radiation and Isotopes, Vol. 23, 1972
[4] "Krypton-85: A Review of Instrumentation for Environmental Monitoring," Robert J. Budnitz, Lawrence Berkeley Laboratory LBL-1779
[5] Eqn. 9.25 "Beta Decay," **Introductory Nuclear Physics**, Chapter 9, p. 272, Kenneth S. Krane, John Wiley & Sons, 1987.
[6] http://www-nds.iaea.org/relnsd/vcharthtml/VChartHTML.html]
[7] "Modeling Ionizing Radiation Induced Gain Degradation of the Lateral PNP Bipolar Junction Transistor," D.M. Schmidt, et al, IEEE Transaction of Nuclear Science, Vol. 43, No. 6, Dec. 1996.
[8] "Using Laboratory X-ray and Cobalt-60 Irradiations to Predict CMOS Device Response in Strategic and Space Environments," D.M. Fleetwood, et al, IEEE Transaction of Nuclear Science, Vol. 35, No.6, Dec. 1988.